Textile UHF-RFID Antenna Sensor for Measurements of Sucrose Solutions in Different Levels of Concentration

Chengyang Luo, Ignacio Gil and Raúl Fernández-García

Department of Electronic Engineering, Universitat Politecnica de Catalunya, Barcelona 08222, Spain

E-mail: chengyang.luo@upc.edu

April 2021

Abstract. With the trend of textile antennas development, Ultra High Frequency (UHF, 865-868 MHz) Radio Frequency Identification (RFID) devices using textile materials are expected to be developed in many areas for replacing or simplifying some complex RFID devices on a PCB. In this paper, we present a textile UHF-RFID tag with two sensing positions ('radiation parts' and 'loop part') for exploring the feasibility of sucrose solutions measurements and the relationship between variables of the proposed design and the sucrose solutions. The simulated and measured resonance curves of the designs both match well (-20 dB in the simulation and -15.8 dB in the measurement at 868 MHz) and the read range measured by the RFID reader (M6e kit) is 1.71 m in air. Before the tests by the solutions on the proposed designs, a test board is developed as a preparation work for confirming the relative dielectric constants of the sensing substrate area in the real measurements. Compare the results of the simulation and the real tests, the proposed design shows good feasibility by comparing the simulated and measured results in confirmed relative dielectric constants. Moreover, its two sensing positions have different sensing features. The sensing 'radiation parts' position shows a stable frequency operation performance but sensing range is from 1.71 m (dry) to 2.3 m, while the sensing 'loop part' position has a wide sensing range from 0.4 m to 1.71 m (dry) but a lower frequency operation performance.

Keywords: textile, Radio Frequency Identification (RFID), Utral High (UHF) frequency, sucrose solution, concentration, read range, relative dielectric constant

1. Introduction

In modern society, Radio Frequency Identification (RFID) technology is essential in diverse applications [1][2][3] such as the goods classification, industrial process monitoring [4], transportation [5], localization and stuff management [21]. Most of them with popular integrated circuit (IC) chips are developed on a hard or flexible Printed Circuit Board (PCB). Due to the physical features of the commercial PCBs, most of RFID tags on a PCB are used as a ID tag, while when for sensing applications

they are normally designed to connect to specifical sensors [6]. In addition, for sensing applications, RFID sensors on a PCB are often used in common fields such as temperature monitoring [7], brightness detection [8] and pressure measurements [9]. In order to expand application fields, some studies focused on RFID tags with chemical sensors [10][11], providing researchers more inspiration to explore the RFID technology on others materials with the similar features of physical or chemical sensors.

In recent years, textile materials are obtaining more attention due to its special features such as flexibility, hygroscopicity and comfort according to the aforementioned background. Current RFID antenna designs deployed on textile materials involve two main approaches, one of which is a copper-based RFID antenna printed on a textile substrate [12][13][14][15], another of which is the metal-plated yarns sewed on a textile substrate [16][17][18][19]. Some of them focus on feasibility [13][14][15], reliability [17][18][19] and common applications such as tracking [16]. Especially for the work [12], the design is based on a copper antenna and a polyimide substrate which is applied for sensing solutions in the liquid through sensitivity (read power) of the RFID tag as the sensing parameter. It is a good idea and deserved to be referred for some RFID antenna sensor designs based on complete textile materials which offer the advantage of being more sensitive to liquids due to the conductive yarns in comparison with normal copper designs. Moreover, some works [18][19] are based on NFC technology operating at 13.5 MHz, which mainly uses capacitive or inductive coupling ways for sensing and is different with UHF-RFID technology based on backscattering [20]. Compared with the common Ultra High Frequency (UHF, 865-868 MHz) RFID tags and sensors on a PCB, the majority of textile UHF-RFID tags and sensors are embroidered by conductive yarns on textile substrates [20][22], which is more different than the copper on PCB. On the one hand, the textile tags can be deployed on common clothes which are more comfortable and lighter than those based on PCB inserted into clothes. On the other hand, the conductive yarns and textile substrates are sensitive to the environmental factors such as humidity [23], temperature, bending and washing [24][25]. As a result, textile UHF-RFID sensors can be explored to replace or simplify some complex or expensive UHF-RFID sensors on the PCB.

Comparing with some studies using chemical sensors on a PCB for the target of wireless sweat-based monitoring [26], some textile materials with better hygroscopicity are expected to reach same target by supporting conductive-yarns-plated UHF-RFID tags. In addition, based on our previous study on solutions sensing [27], the textile UHF-RFID sensor based on only tags is promising to be explored gradually.

In this paper, the textile UHF-RFID tag with two sensing positions ('radiation parts' and 'loop part') is proposed for sucrose solution measurements. Considering the possibility of expending future sensing applications, the function-extensible IC chip (ROCKY 100) is used in the proposed design. Before the tests on proposed textile UHF-RFID sensor, a test board is developed in the preparation work for confirming the relative dielectric constants of the sensing substrate area in the real measurements. The fundamental resonance analysis for the simulated and measurements is performed.

Then in order to explore the relationship between variables of the proposed design and the sucrose solutions, two sensing positions are used to absorb the sucrose solutions with different levels of concentration. Then the read ranges of the design in different situations are tested by a RFID reader (M6e Kit) and analyzed combined with simulated results after obtaining the real relative dielectric constants of the sucrose solutions by the preparation work.

2. Design and Related Details

2.1. Structure of the proposed textile UHF-RFID antenna

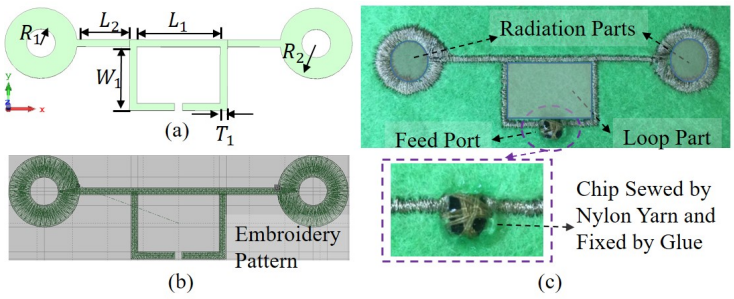

Figure 1. Geometry and configuration of the proposed design. (a) simulated design diagram, (b) embroidered pattern diagram, (c) photograph of the proposed design

The geometry and configuration of the proposed textile UHF-RFID antenna sensor are shown in Fig. 1.The design mainly consists of two parts which are the 'loop part' for impedance match and the 'radiation parts' for improving the transmit-receive ability as shown in Fig. 1 (c). In Fig. 1 (a), the simulated design is presented and related size parameters are detailed in Table. 1. Note that when the design is embroidered by specific machines, the embroidery pattern makes certain influence on the impedance of the textile UHF-RFID antenna. As a result, the proposed design is converted to an embroidery pattern by 'satin fill' mode as shown in Fig. 1 (b).

In addition, for the UHF-RFID integrated circuit (IC) chip, a ROCKY 100 is selected due to its function-extensible feature. Comparing with some popular chips for textile RFID tags such as Monza R6, the ROCKY 100 can extend functions by connecting to various sensors. Certainly, in this paper, the proposed textile UHF-RFID tag is explored to be an antenna sensor without sensors expansion. The complex impedance of the used chip (ROCKY 100) is 64-i*469 ohm and the minimum wake-up power is -10 dB. For conjugate matching, the impedance of the feed port in simulation software needs to be set as 64+i*469 ohm.

2.2. Materials

The proposed textile UHF-RFID antenna sensor is embroidered using conductive yarns as the antenna sensor and polyester fibers as the substrate. The textile material of the

Table 1. Size parameters of the design (Unit: mm)

Parameter	L_1	L_2	W_1	T_1	R_1	R_2
Value	23	14.5	18	2	4	10

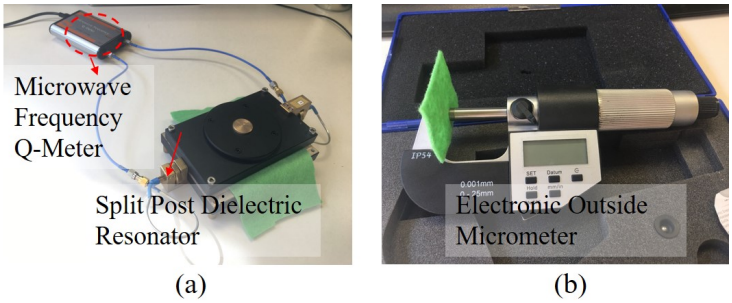

Figure 2. Substrate parameters measurements. (a) Permittivity and loss tangent measurements, (b) Thickness measurement.

antenna is a commercial conductive twisted yarn (Shieldex 117/17 dtex 2-ply) made of 99% pure silver-plated Nylon. Note that in order to reduce the impact from the difference between the pure silver and the real silver-plated Nylon[28][29], the most closed bulk conductivity of the yarns is redefined as 11500 siemens/m in the simulation software.

Moreover, the polyester [30] is selected as the substrate due to its better hygroscopicity. Its relative dielectric constant and loss tangent in a dry situation are 1.24 and 0.000163, respectively, measured by a Microwave Frequency Q-Meter as shown in Figure 2 (a). On the other hand, its thickness is 0.62 mm measured by an Electronics Outside Micrometer (132-01-040A) as shown in Figure 2 (b).

Considering the textile materials have the special feature (better hygroscopicity than PCBs), the solutions in different levels of concentration are expected to make an impact on substrate performance. In next section, this impact is evaluated.

3. Tests and Achieved Results

Resistance and reactance curves for antennas have bigger slopes in the curve-rising stage, which means the resistance and reactance values change sensitively. Hence, when the design is used to absorb certain solutions causing change of substrate ε_r, some electrical properties such as the resonance frequency and read range are expected to change. In this section, the related tests are done for exploring the viability of the prototype as a sensor and relationship between variables.

The measurement procedures of the whole work are divided into two parts linked by the special 'medium' as shown in Fig. 3. The first part is the preparation test and the second part is the UHF-RFID antenna sensor test. In detail, a simple capacitive structure is developed by means of simulation software and embroidered by

the aforementioned embroidery machine. The S-parameter curves of the simulation and the real measurements are expected to be matched to obtain the corresponding values of ε_r as the fitting parameter. The obtained values ε_r related to the solution concentration are used in the UHF-RFID sensor simulation of the second part and then the simulated results are compared with the measured results to confirm the feasibility of the measurement method by the textile UHF-RFID sensors. Note that the ε_r is the bridge or medium to connect the first and second parts as shown in Fig. 3.

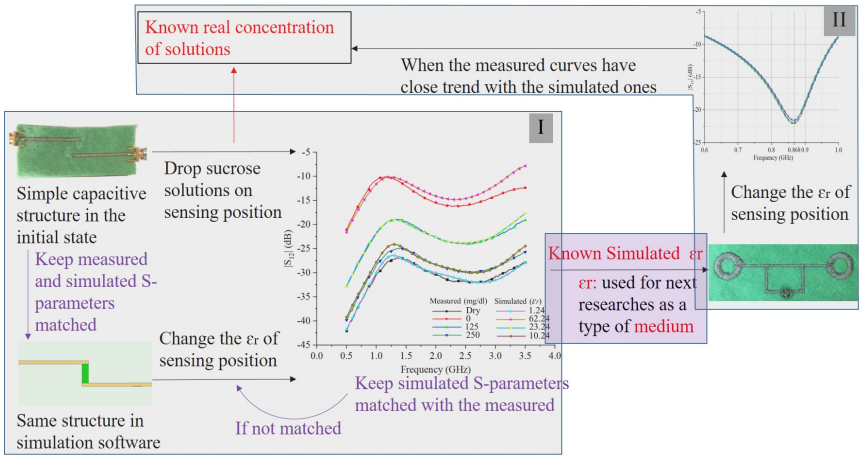

Figure 3. Measurement procedures of the whole work

3.1. Preparation Test

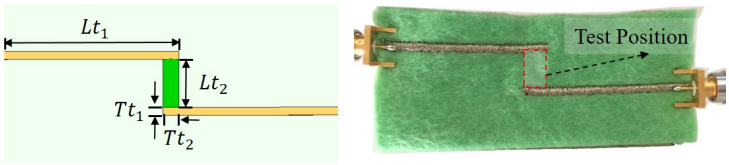

Figure 4. Geometry and configuration of the test board. (a) simulated test board diagram, (b) photograph of the test board

In order to confirm the real relative dielectric constants of the sensing areas of the proposed design in different situations for validating the feasibility to be a wireless sensor for the concentration measurement of sucrose solutions, a preparation test is conducted in this section.

As shown in Fig. 4, the same textile-based test board is designed by a professional embroidery machine (Singer Futura XL-550) to measure the real relative dielectric constants of the sensing areas with the sucrose solutions [32] in the different levels of concentration. The Fig. 4 (a) depicts the simulated test board model which is

Table 2. Size parameters of the test board (Unit: mm)

Parameter	L_{t1}	L_{t2}	T_{t1}	T_{t2}
Value	44	12	2	2

embroidered by the mentioned method as shown in Fig. 4 (b). In addition, the related size parameters are given in the Table. 2.

Moreover, the sucrose solutions are prepared by distilled water and sucrose (0, 125 mg/dl and 250 mg/dl). In order to obtain the sucrose solutions with different levels of concentration, accurate weighing is done for the sucrose by a precise balance (PCE-BS 300).

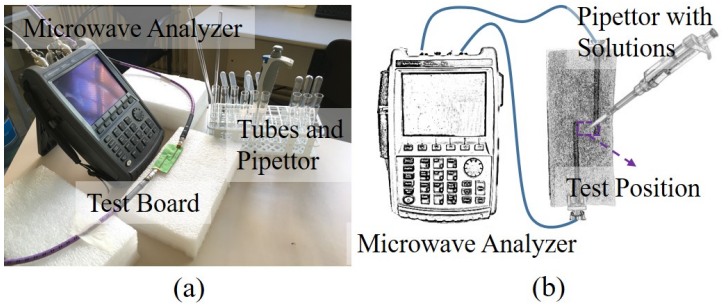

Figure 5. Measurement setup for the preparation test. (a) Photograph of measurement setup, (b) Measurement setup configuration.

The measurement setup for the preparation test is shown in Fig. 5 and the test procedure is listed as follows,

(i) Connect the two ports of the test board to the Microwave Analyzer N9916A as shown in Figure 5 (a), and save the reflection coefficients of the test board in dry conditions.

(ii) Compare the saved data from first step with the simulated curves of the test board model and confirm the both are matched.

(iii) Drop the sucrose solutions in different levels of concentration (0, 125 mg/dl and 250 mg/dl) onto the sensing position of the test board, and save the reflection coefficients in each situation.

(iv) Adjust the relative dielectric constants of the sensing area in the simulation software to find the matched curves with the measured curves. The corresponding relative dielectric constants are closed to the real relative dielectric constants of the sensing substrate area in the real measurements.

By the above test procedure, the test results are shown in Fig. 6 and Fig. 7. From the experimental results, the relative dielectric constants of the sensing substrate area tuned to 62.24, 23.24 and 10.24 for 0, 125 mg/dl and 250 mg/dl, respectively. Therefore,

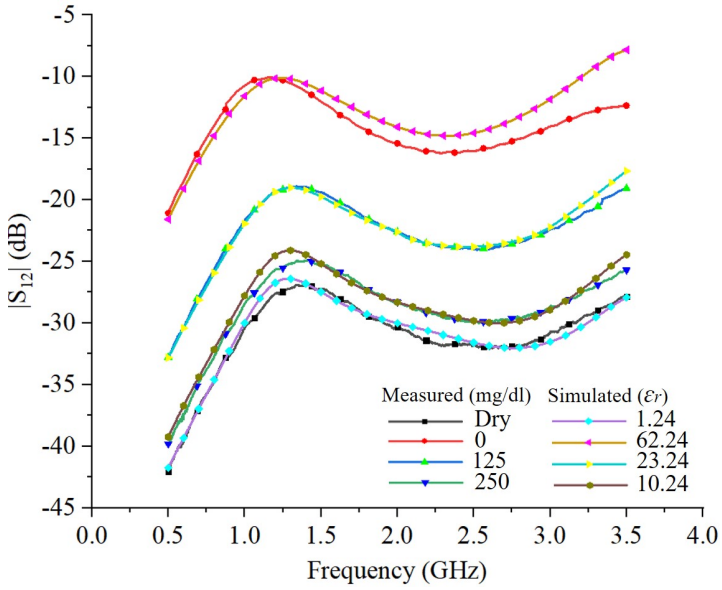

Figure 6. Simulated and measured $|S_{12}|$ of the test board for measuring the relative dielectric constant of the tested position with solutions.

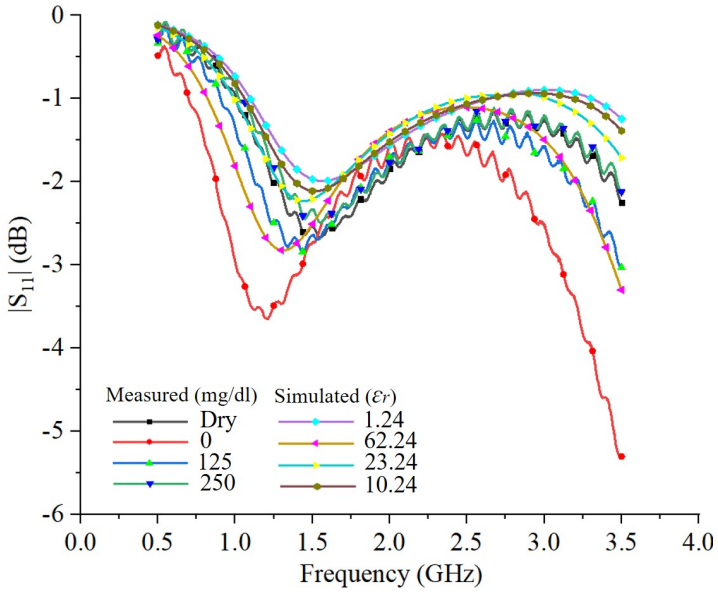

Figure 7. Simulated and measured $|S_{11}|$ of the test board for measuring the relative dielectric constant of the tested position with solutions.

the obtained relative dielectric constants can be used for the proposed design in next sensing tests.

3.2. Resonance analysis

Fig. 8 shows the simulated and measured reflection coefficients ($|S_{11}|$) of the embroidered UHF-RFID antenna, in which the measured curve is obtained by Microwave Analyzer N9916A with 'port extension' function. The simulated $|S_{11}|$ reaches -22 dB at resonance

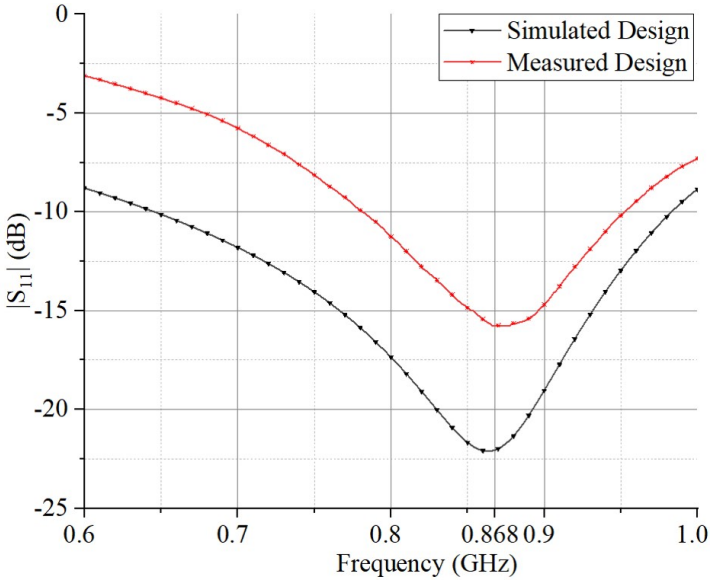

Figure 8. Simulated and measured reflection coefficients of the embroidered designs in a dry condition.

frequency 868 MHz and the bandwidth under -10 dB is 337 MHz from 646 MHz to 983 MHz. Comparing with the simulated result, the measured $|S_{11}|$ is a little different, which shows -15.8 dB at 868 MHz and 170 MHz of the bandwidth from 782 MHz to 952 MHz. From the results, the design can work at targeted ultra high resonance frequency (868 MHz).

3.3. Tests under sucrose solutions in different levels of concentration

Considering the specifical features of the proposed textile UHF-RFID tag such as the sensitive impedance change and the better substrate hygroscopicity than that of a common PCB,the sucrose solution for the proposed textile UHF-RFID tag is selected to explore the possibility as a sensor and the relationship between the concentration and the read ranges. For the proposed design, there are two positions selected as the sensing areas, the 'radiation parts' and the 'loop part' as shown in Fig. 1 (c). The two positions are analyzed with respect to the Friis Transmission Formula as follows [13][31],

$$d_{max} = \frac{\lambda}{4\pi}\sqrt{\frac{P_t G_t G_r \cdot \tau}{P_{th}}} \tag{1}$$

where d_{max} is the maximum value of the read range, λ is the wave length at 868 MHz, P_t is the power fed into the reader antenna, G_t is the gain of the reader antenna, G_r is the gain of the proposed antennas, τ is the largest power transmission coefficient and P_{th} is the minimum wake-up power of the chip.

From the equation 1, the maximum value of the read range (d_{max}) can be affected by the gain of the proposed antenna (G_r) and the largest power transmission coefficient (τ). Therefore, the 'radiation parts' and the 'loop part' related to the G_r and τ, respectively,

are good choices. When the solutions with different levels of concentration are dropped on the sensing areas, the relative dielectric constants of the sensing areas are expected to change. The measured relative dielectric constants of the sensing area in different levels of concentration are confirmed in the preparation test above.

· Tests at the 'radiation parts' position

The reflection coefficients ($|S_{11}|$) are simulated by sweeping the relative dielectric constant of the substrate at only the 'radiation parts' and the results at ε_r=1.24 (dry), ε_r=10.24 (250 mg/dl), ε_r=23.24 (125 mg/dl) and ε_r=62.24 (0 mg/dl) are selected to compare with the real measurement results.

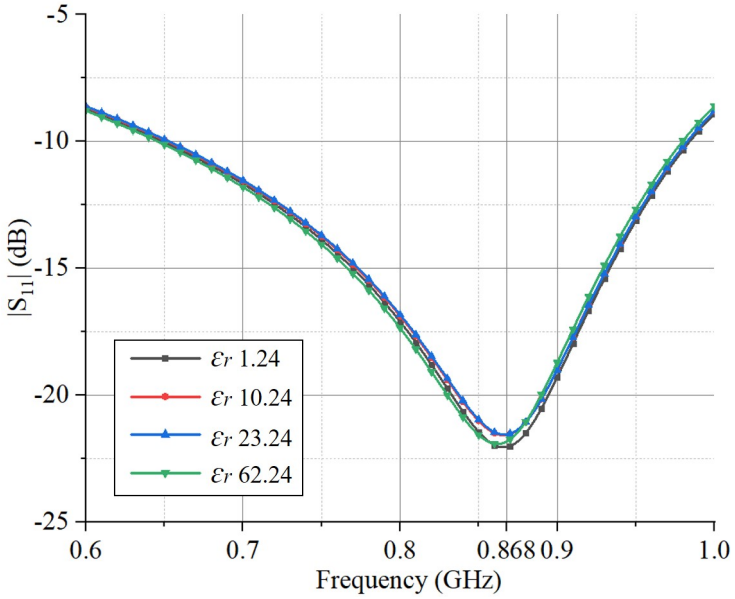

Figure 9. Simulated reflection coefficients of the proposed design with different relative dielectric constants at two 'radiation parts' positions.

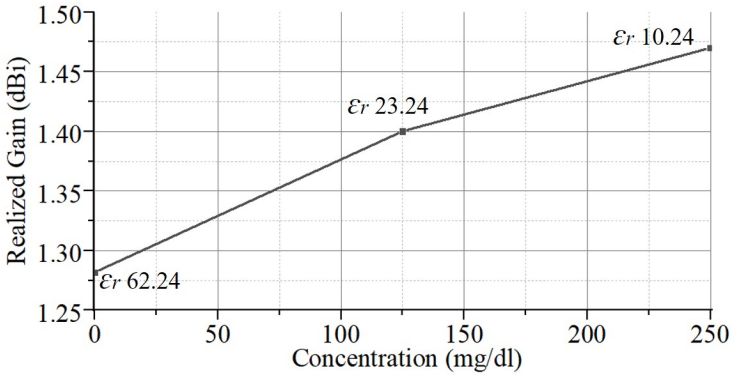

Figure 10. Simulated realized gain at 868 MHz of the proposed design with different relative dielectric constants at the two 'radiation parts' positions.

As shown in Fig. 9, all $|S_{11}|$ curves are close, which means when using 'radiation

parts' to measure the sucrose solutions, the resonance frequency is expected to be stable. Meanwhile, as shown in Fig. 10, the realized gain curve including all situations (ε_r: 10.24, 23.24 and 62.24) shows an increase in the target concentration range from 0 to 250 mg/dl. In addition, the realized gain in a dry situation (ε_r: 1.24) reaches 0.9 dBi, which means comparing to the results in wet situations the realized gain is expected to increase when sensing the solutions.

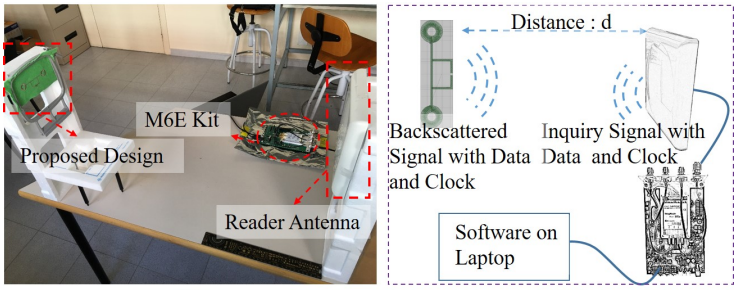

Figure 11. Measurement setup for the read ranges of the embroidered designs when sensing solutions. (a) Photograph of measurement setup, (b) Measurement setup configuration

According to equation 1, the maximum read range is related to the six factors including λ, P_t, G_t, G_r, τ and P_{th}. There are four of them (λ, P_t, G_t and P_{th}) which are determined by the resonance frequency (868 MHz in the work), EIRP (Europe, P_tG_t=2 W), RFID IC chip (Rocky 100 in the work, P_{th}=-10 dBm). However, the G_r, τ are determined by the UHF-RFID antenna.

When the match situations (τ)are close as shown in Fig. 9, the simulated read range curve has a linear relationship with the square root of simulated realized gain (liner values not dB value) as Equation 2 shows,

$$d_{max} \propto \sqrt{G_r} \tag{2}$$

Table 3. Tests and validation results on 'radiation parts'

Test Points				*Validation Points*	
Concentration (mg/dl)	0	125	250	75	175
Read Power 1st (dBm)	12.1	11	10.5	11.3	10.8
Read Power 2nd (dBm)	12.1	10.9	10.6	11.4	10.8
Read Power 3rd (dBm)	11.9	11.1	10.4	11.3	10.7
Read Power 4th (dBm)	12	11	10.5	11.3	10.8
Average Read Power (dBm)	12	11	10.5	11.3	10.8
Read Range (m)	1.926	2.161	2.289	2.087	2.211

In order to validate the trend and explore the sensing ability, the real design embroidered by the same embroidery mode with the test board ('satin fill') is tested

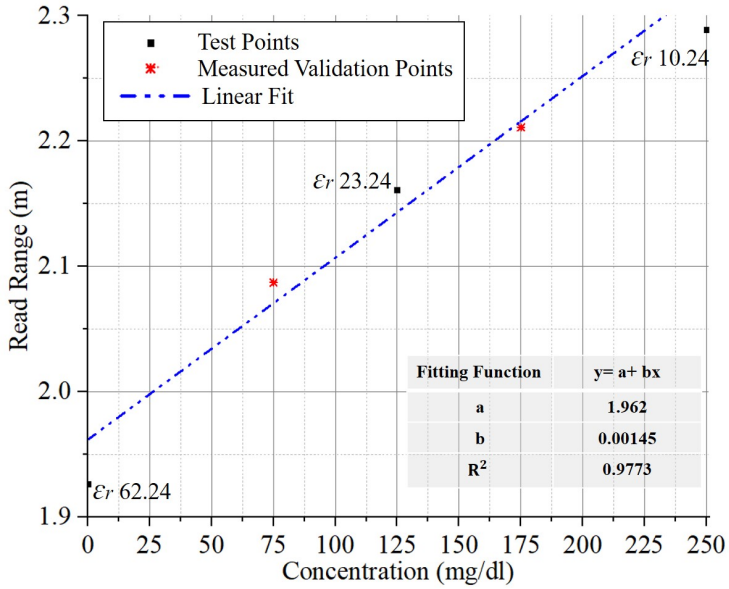

Figure 12. Measured read range at 868 MHz of the proposed design dropped by sucrose solutions at the 'radiation parts'.

Table 4. Error between the measured validation points and the fitting curves

Read Range (m)	*Concentration (mg/dl)*	
	75	175
Validation Points	2.087	2.211
Linear Fit	2.071	2.216
|Error|	0.016	0.005

by sucrose solutions in different levels of concentration (0, 125 mg/dl and 250 mg/dl) at the 'radiation parts'. The read range can be measured by a RFID reader with a reader antenna (MT-242025/TRH/A/A) controlled by the M6E Kit as shown in Fig. 11.

The tests on 'radiation parts' as shown in Fig. 11 are conducted for 4 times and final read powers are obtained by calculating average value as shown in Table 3. Note that the distance between the design and the read antenna is set to 0.35 m and the read range can be calculated by using the Equation 1.

To explore the trend of the real read range, the linear fit is adopted. In addition, in order to validate the trend of the measurement curve, the solutions in the concentration of 75 mg/dl and 175 mg/dl are detected. All the results are shown in Fig. 12.

As shown in Fig. 12, the measured read range rises as the concentration goes up, but all the values in wet situations are higher than that when the sensing position is dry. Note that the relative dielectric constants of the sucrose solution decrease as the levels of concentration increase[32][33]. The measured validation points are close to the fitting curve as shown in Table 4, which confirm the feasibility and availability of the measurement curves and method. In addition, by comparing the two figures, Fig. 10 and Fig. 12, the measured results trend that all the values in wet situations are higher

than that in dry situation match with the trend of the simulated realized gain curve.

· Tests at the 'loop part' position

The same tests are conducted on the 'loop part'. As shown in Fig. 13, the resonance frequency shift left gradually as the relative dielectric constants (ε_r) increase continuously. However, only the curves whose (ε_r) is below 23.24 have the $|S_{11}|$ below -10 dB at 868 MHz. In other words, when using 'loop part' to measure the sucrose solutions, the performance of the textile UHF-RFID antenna sensor decreases as the levels of concentration are fairly low. Meanwhile, as shown in Fig. 14, the realized gain curve including all situations (ε_r: 10.24, 23.24 and 62.24) shows an continuous decease in the target concentration range from 0 to 250 mg/dl.

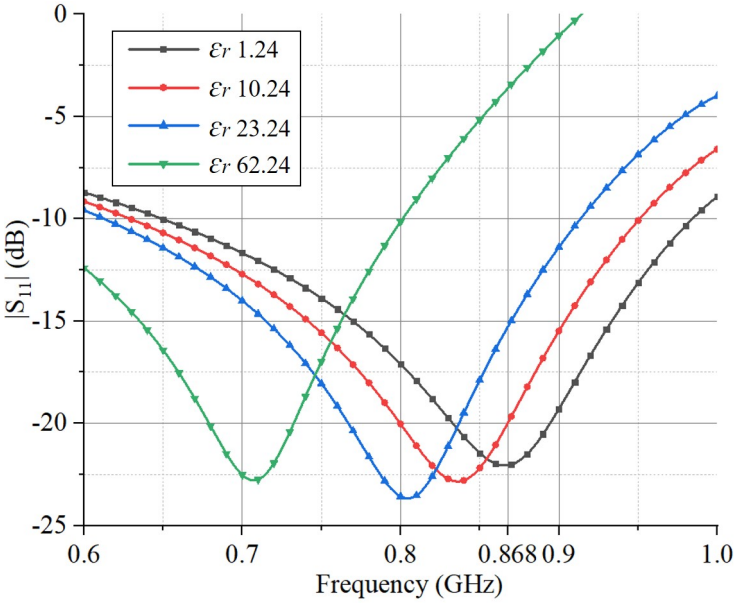

Figure 13. Simulated reflection coefficients of the proposed design with different relative dielectric constants at the 'loop part'.

As aforementioned, the G_r, τ are determined by the UHF-RFID antenna, one of which in this situation, τ, can be calculated by Equation 3,

$$\tau = \frac{4R_{ant}R_{ic}}{(|Z_{ant} + Z_{ic})^2} \tag{3}$$

where R_{ant} is the resistant part of the antenna impedance, R_{ic} is the resistant part of the IC chip impedance, Z_{ant} is the antenna impedance and Z_{ic} is the IC chip impedance. When λ, P_t, G_t and P_{th} are determined, the relationship between the maximum read range and the antenna is obtained as Equation 4 shows,

By calculation, the results can be obtained as shown in the Table 5,

$$d_{max} \propto \sqrt{G_r \cdot \tau} \tag{4}$$

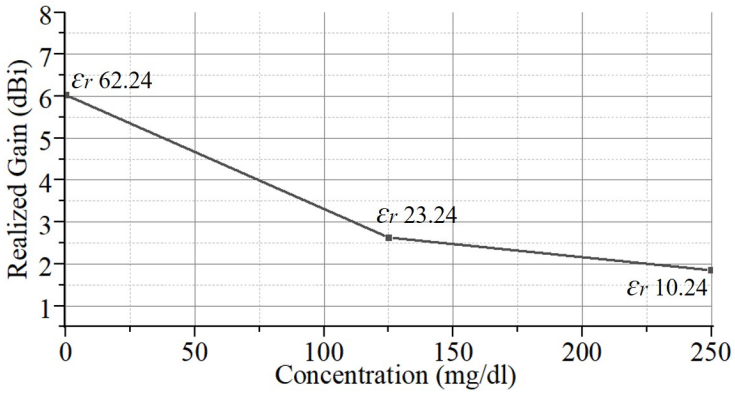

Figure 14. Simulated realized gain at 868 MHz of the proposed design with different relative dielectric constants at the 'loop part'.

Table 5. Realized gain data and calculated results

ε_r	10.24	23.24	62.24
G_{rdbi}/DBi	1.8472	2.6324	6.0251
$G_r(linear\ value)$	1.5301	1.8333	4.0041
τ	0.8126	0.6354	0.2043
$\sqrt{G_r} \cdot \sqrt{\tau}$	1.115	1.0793	0.9045

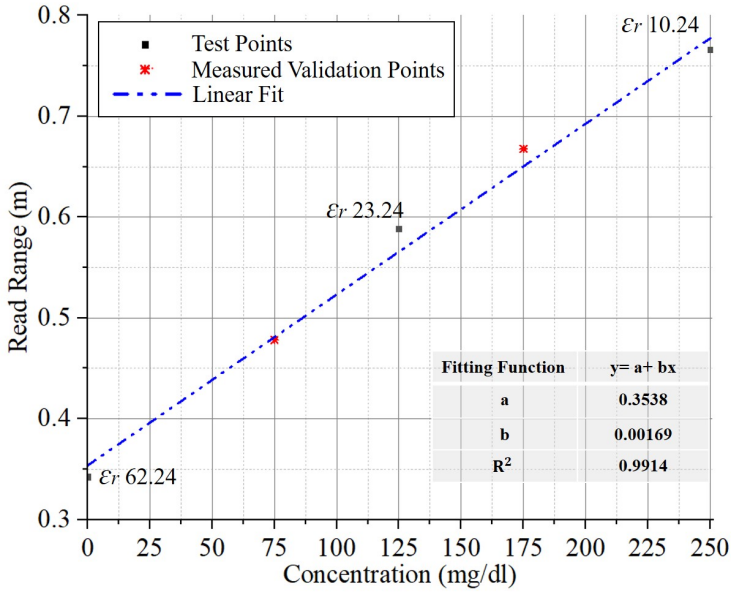

Figure 15. Measured read range at 868 MHz of the proposed design dropped by sucrose solutions at the 'loop part'.

Table 6. Tests and validation results on 'loop part'

Test Points				*Validation Points*	
Concentration (mg/dl)	0	125	250	75	175
Read Power 1st (dBm)	27	22.3	20.1	24.1	21.3
Read Power 2nd (dBm)	27.2	22.1	19.9	24	21.3
Read Power 3rd (dBm)	27.1	22.4	19.8	24.2	21.1
Read Power 4th (dBm)	26.8	22.3	20	24.1	21.2
Average Read Power (dBm)	27	22.3	20	24.1	21.2
Read Range (m)	0.3424	0.5365	0.766	0.4782	0.6677

Table 7. Error between the measured validation points and the fitting curves

Read Range (m)	*Concentration (mg/dl)*	
	75	175
Validation Points	0.4782	0.6677
Linear Fit	0.4806	0.6496
|Error|	0.0024	0.0181

The read range of the real embroidered design is also tested by sucrose solutions in different levels of concentration (0, 125 mg/dl and 250 mg/dl) at the 'loop part' and measured by the RFID reader. As shown in Fig. 15, the measured read range rises as the concentration goes up, but all the values in wet situations are lower more than that when the sensing position is dry.

The tests on 'loop part' as shown in Fig. 11 are conducted for 4 times and final read powers are obtained by calculating the average value as shown in Table 6. Note that the certain distance between the design and the read antenna is set to 0.35 m and the read range can be calculated by using the Equation 1.

To explore the trend of the real read range, the linear fit is adopted. In addition, in order to validate the trend of the measurement curve, the solutions in the concentration of 75 mg/dl and 175 mg/dl are detected. All the results are shown in Fig. 15. Moreover, the measured validation points are close to the fitting curve as shown in Table. 7, which confirm the feasibility and availability of the measurement curves and method.

In addition, by comparing the Table 5 and Fig. 15, the measured results that all the values in wet situations are lower than that in dry situation match with the simulated results. The reason for the opposite trends of the realized gain curve and the read range curve is that the shifting resonance frequency (different match situations) presents a bigger influence on the read range than the affecting factor from the realized gain.

Moreover, by analyzing the curves with the relative dielectric constants (10.24, 23.24 and 62.24) in Fig. 10 and Fig. 14 compared with the measured read range results in Fig. 12 and Fig. 15, the trends in real measurements are matched with the simulated trends and the sensing feasibility of the proposed textile UHF-RFID antenna is confirmed.

The proposed textile UHF-RFID antenna sensor has the feasibility to be a wireless sensor for the concentration measurement of sucrose solutions. In addition, another novel point is that the proposed design has two sensing positions, the 'radiation parts' and the 'loop part'. The two sensing positions have different advantages, one of which ('radiation parts') have a stable operation performance but sensing range is from 1.71 m (dry) to 2.3 m (current measured solutions), while another of which ('loop part') have a wide sensing range from 0.4 m (current measured solutions) to 1.71 m (dry) but a lower operation performance. The two choices can be adopted with respect to different applications.

4. Conclusion

To conclude, a textile UHF-RFID antenna sensor with the two sensing positions ('radiation parts' and 'loop part') is developed. To explore the possibility for textile UHF-RFID tag as a sensor and relationship between variables, the proposed design has been tested by sucrose solutions in different levels of concentration (0, 125 mg/dl and 250 mg/dl) comparing with the dry situation. Before the tests on the proposed design, the test board is developed in the preparation work for confirming the relative dielectric constants of the sensing substrate area in the real measurements (62.24, 23.24 and 10.24 for 0, 125 mg/dl and 250 mg/dl, respectively). The simulated and measured resonance curves of the proposed designs both match well (-20 dB in the simulation and -15.8 dB in the measurement at 868 MHz) and the read range measured by the RFID reader (M6e kit) is 1.71 m in air. After simulation and real tests, the proposed design used for sensing the sucrose solutions shows good feasibility by comparing the simulated and measured results. Moreover, its two sensing positions have different sensing features. The sensing 'radiation parts' shows a stable frequency operation performance but sensing range is from 1.71 m (dry) to 2.3 m (current measured solutions), while the sensing 'loop part' have a wide sensing range from 0.4 m (current measured solutions) to 1.71 m (dry) but a lower frequency operation performance. The sensing features give future complete application two choices.

Acknowledgments

This work was supported by Spanish Government-MINECO under Project TEC2016-79465-R and China Scholarship Council No.201908440233.

References

[1] Potyrailo R A, Surman C and Monk D 2011 RFID sensors as the common sensing platform for single-use biopharmaceutical manufacturing *Meas. Sci. Technol.* **22** 082001.

[2] Occhiuzzi C, Paggi C and Marrocco G 2011 Passive RFID Strain-Sensor Based on Meander-Line Antennas *IEEE Trans. Antennas Propag.* **59** 4836-4840.

[3] Yang M, Zhang W and Li L 2017 A Resistance-Type Sensor Based on Chipless RFID *IEEE Trans. Antennas Propag.* **65** 3319-3325.
[4] Shafiq Y, Gibson J S, Kim H, Ambulo C P, Ware T H and Georgakopoulos S V 2019 A Reusable Battery-Free RFID Temperature Sensor *IEEE Trans. Antennas Propag.* **67** 6612-6626.
[5] Wang Y, Pretorius A J and Abbosh A M 2016 Low-Profile Antenna With Elevated Toroid-Shaped Radiation for On-Road Reader of RFID-Enabled Vehicle Registration Plate *IEEE Trans. Antennas Propag.* **64** 1520-1525.
[6] Deng F, He Y and Wu X 2014 A CMOS pressure sensor with integrated interface for passive RFID applications *Meas. Sci. Technol.* **25(12)** 125104.
[7] Vaz A, Ubarretxena A and Zalbide I 2010 Full passive UHF tag with a temperature sensor suitable for human body temperature monitoring *IEEE Trans. Circuits Syst. II Express Briefs* **57** 95-99.
[8] Falco A, Salmerón J F and Loghin F C 2017 Fully printed flexible single-chip RFID tag with light detection capabilities *Sensors* **17** 534.
[9] Kuhn M F, Breier G P and Dias A R P 2018 A novel RFID-based strain sensor for wireless structural health monitoring *J. Nondestr. Eval.* **37** 1-10.
[10] Zampolli S, Elmi I and Cozzani E 2018 Ultra-low-power components for an RFID Tag with physical and chemical sensors *Microsyst. Technol.* **14(4-5)** 581-588.
[11] Manzari S, Catini A and Pomarico G 2014 Development of an UHF RFID Chemical Sensor Array for Battery-Less Ambient Sensing *IEEE Sens. J.* **14** 3616-3623.
[12] Ennasar, M.A., El Mrabet, O., Mohamed, K. and Essaaidi, M. 2019 Design and characterization of a broadband flexible polyimide RFID tag sensor for NaCl and sugar detection. Prog. Electromagn. Res. 94 273-283.
[13] Le D, Ahmed S and Ukkonen L 2021 A Small All-Corners-Truncated Circularly Polarized Microstrip Patch Antenna on Textile Substrate for Wearable Passive UHF RFID Tags. IEEE J. Radio Freq..
[14] Manzari S, Occhiuzzi C and Marrocco G 2012 Feasibility of body-centric systems using passive textile RFID tags. IEEE Trans. Antennas Propag. 54 49-62.
[15] Ginestet G, Brechet N and Torres J 2016 Embroidered antenna-microchip interconnections and contour antennas in passive UHF RFID textile tags. IEEE Antennas Wirel. Propag. Lett. 16 1205-1208.
[16] Liu Y, Yu M and Xia B 2021 E-Textile Battery-less Displacement and Strain Sensor for Human Activities Tracking. IEEE Internet Things J.
[17] Liu Y, Xu L and Li Y 2019 Textile based embroidery-friendly RFID antenna design techniques IEEE International Conference on RFID 1-6.
[18] Escobedo P, de Pablos-Florido J and Carvajal M A 2020 The effect of bending on laser-cut electro-textile inductors and capacitors attached on denim as wearable structures. Text. Res. J. 90 2355-2366.
[19] Jiang Y, Xu L and Pan K 2019 e-Textile embroidered wearable near-field communication RFID antennas. IET Microw. Antennas Propag. 13 99-104.
[20] Luo C, Gil I and Fernández-García R 2020 Wearable textile UHF-RFID sensors: A systematic review. Materials, 13 3292.
[21] Ali Z, Perret E and Barbot N 2020 Authentication Using Metallic Inkjet-Printed Chipless RFID Tags *IEEE Trans. Antennas Propag.* **68** 4137-4142.
[22] Koski K, Sydänheimo L and Rahmat-Samii Y 2014 Fundamental Characteristics of Electro-Textiles in Wearable UHF RFID Patch Antennas for Body-Centric Sensing Systems *IEEE Trans. Antennas Propag.* **62** 6454-6462.
[23] He H, Chen X and Khan Z 2020 Textile-based Passive Sensor for Air Humidity *2020 IEEE 8th Electronics System-Integration Technology Conference (ESTC)* 1-3.
[24] Fu Y Y, Chan Y L and Yang M H 2015 Experimental Study on the Washing Durability of Electro-Textile UHF RFID Tags *IEEE Antennas Wirel. Propag. Lett.* **14** 466-469.
[25] Simorangkir R B V B, Le D and Björninen T 2019 Washing Durability of PDMS-Conductive

Fabric Composite: Realizing Washable UHF RFID Tags *IEEE Antennas Wirel. Propag. Lett.* **18** 2572-2576.

[26] Gao W, Emaminejad S and Nyein H Y Y 2016 Fully integrated wearable sensor arrays for multiplexed in situ perspiration analysis *Nature* **529** 509–514.

[27] Luo C, Fernández-García R and Gil I 2020 Embroidered Textile Capacitive Sensor for Sucrose Solutions Measurement," *2020 IEEE International Conference on Flexible and Printable Sensors and Systems (FLEPS)* 1-4.

[28] Zhang H 2015 Flexible textile-based strain sensor induced by contacts *Meas. Sci. Technol.* **26(10)** 105102.

[29] Logothetis I, Bayramol D V and Gil I 2020 Evaluating silver-plated nylon (Ag/PA66) e-textiles for bioelectrical impedance analysis (BIA) application *Meas. Sci. Technol.* **31(7)** 075101.

[30] http://www.urbatex.com/en/tessuto/polyester-fabric/

[31] Deleruyelle, T., P. Pannier, M. Egels, and E. Bergeret 2010 Dual band mono-chip HF-UHF tag antenna Proc. IEEE Antennas Propag. Soc. Int. Symp. 1–4.

[32] Malmberg C G and Maryott A A 1950 Dielectric constants of aqueous solutions of dextrose and sucrose *Journal of Research of the National Bureau of standards* **45** 299-303.

[33] Harnsoongnoen S and Wanthong A 2015 Coplanar waveguides loaded with a split ring resonator-based microwave sensor for aqueous sucrose solutions *Meas. Sci. Technol.* **27(1)** 015103.